

Nanomechanical electron shuttle consisting of a gold nanoparticle embedded within the gap between two gold electrodes

Andriy V. Moskalenko,¹ Sergey N. Gordeev,^{1,*} Olivia F. Koentjoro,² Paul R. Raithby,² Robert W. French,² Frank Marken,² and Sergey E. Savel'ev³

¹Department of Physics, University of Bath, Claverton Down, Bath BA2 7AY, United Kingdom

²Department of Chemistry, University of Bath, Claverton Down, Bath BA2 7AY, United Kingdom

³Department of Physics, Loughborough University, Loughborough LE11 3TU, United Kingdom

(Received 15 May 2009; published 22 June 2009)

Nanomechanical shuttles transferring electrons from one electrode to another, in groups or individually, offer a solution to the problem of controlled charge transport. We report the fabrication of shuttle junctions consisting of a gold nanoparticle embedded within the gap between two gold electrodes and attached to them through a monolayer of molecular “springs.” When a voltage bias is applied, the nanoparticle starts to oscillate, transferring electrons from one electrode to the other. Measured I - V characteristics have been compared with the results of computer simulations.

DOI: 10.1103/PhysRevB.79.241403

PACS number(s): 73.63.-b, 73.23.Hk, 78.67.Bf

In 1998, Gorelik *et al.*¹ proposed a mechanism of charge transport based on shuttling of electrons by an oscillating metallic nanoparticle mechanically coupled via elastic molecules to two nanoelectrodes [see Fig. 1(a)]. For low applied voltages where the nanoparticle is stationary the device is similar to a single-electron transistor (SET).² When a sufficient voltage bias is applied to the electrodes the nanoparticle starts to oscillate, transferring an electrical current $I=2Nef$ that is proportional to the vibration frequency f and the number of electrons N residing on the nanoparticle, which, in turn, depends on the applied voltage and the size of the nanoparticle. One of the potential advantages of the shuttle junctions is that, in contrast to SETs, *only one tunneling barrier is open at a time*.¹ This prevents simultaneous tunneling of two electrons through the barriers (so-called cotunneling effect^{3,4}), thus increasing accuracy of the single-electron transport. Exploitation of the shuttle mechanism could potentially lead to the development of a new generation of nanomechanical electronic devices, such as transistors, current standards, very sensitive electrometers, sensors, logic gates, and memories with ultralow power consumption and high speed of operation.

Interest in electron shuttles and, more generally, in the fundamental properties of electromechanical coupling in nanostructures, initially generated by theoretical papers^{1,5,6} (see also Ref. 7 for a review) has grown tremendously over the last few years⁸⁻¹⁷ as experimentalists made the first attempts at the practical realization of such devices. There were reports about manufacturing of different nanoelectromechanical systems (NEMS) using semiconductor fabrication technology. In these systems the charge transfer was performed by a flexible semiconductor element such as a silicon beam resonator,¹⁸ clamped GaAs beam,¹⁹ cantilever,²⁰ and silicon nanopillar.²¹ However, the functional elements of all these devices are comparatively large (larger than 100 nm), work at a fixed frequency, and usually required an additional ac driving voltage to set up oscillations of the flexible element at its resonant frequency. Very elegant experiments have been performed by Park *et al.*²² who measured electron transport through a molecule of C₆₀ that was trapped

between two electrodes during the electromigration process. However, as C₆₀ molecules are only ~1 nm in diameter, it was impossible to take an image of the molecule inside the nanogap and thus to confirm that the current was indeed transported through a C₆₀ molecule. There are many other electromechanical nanosystems that are currently the subject of intense study by theoreticians and are awaiting practical realizations. These include shuttling of superconducting Cooper pairs^{5,23,24} and spin-polarized electrons.²⁵ In the latter case giant magnetotransmittance effects are predicted.²⁶

In the present work, we describe the fabrication and properties of metallic electromechanical nanoshuttles consisting of a 20 nm gold nanoparticle embedded in the gap between two electrodes and attached to them through a monolayer of flexible organic molecules. We have found that the geometry of shuttle junctions suggested by Gorelik *et al.*¹ [Fig. 1(a)] is very inconvenient from the point of view of fabrication as it

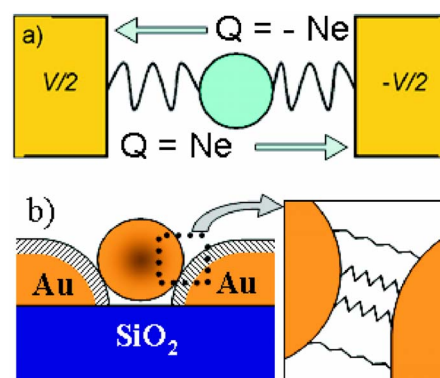


FIG. 1. (Color online) (a) Theoretical model of an idealized shuttle junction and illustration of the shuttling process (Ref. 1) and (b) experimental realization of the shuttle junction. The device consists of a 20 nm gold nanoparticle attached to two gold electrodes through monolayers of octanedithiol molecules serving as springs. The inset in Fig. (b) shows how the nanoparticle is attached to the electrode through a monolayer of elastic molecules; due to the curvature of the particle and electrode, some molecules are over-stretched within the gap.

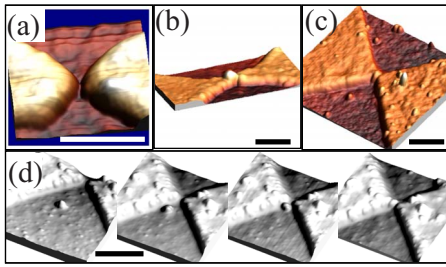


FIG. 2. (Color online) Assembly of shuttle junctions. (a) A pseudo-three-dimensional (3D) atomic force microscope (AFM) image of electrodes used for fabrication of a shuttle junction; (b) and (c) images of fabricated shuttle junctions; and (d) sequence of AFM images taken during manipulation of a 20 nm nanoparticle into the gap between two electrodes. Scale bars are (a) 100 and (b)–(d) 200 nm.

requires a high-precision matching between the size of the gap and the shuttle diameter. To reduce requirements to accuracy of fabrication we have elaborated a structure which is depicted schematically in Fig. 1(b). We fabricated the nanoelectrodes with rounded edges so that small variations in the nanoparticle diameter are less critical than in Fig. 1(a).

Shuttle-junction devices were formed on the top of a silicon wafer coated with a $\sim 1 \mu\text{m}$ SiO_2 layer. Planar 30-nm-thick gold nanoelectrodes separated by a gap of 10–20 nm were fabricated using electron-beam lithography followed by lift-off. When parameters of exposure, metal deposition, and the lift-off process are optimized, this technique gives smooth electrodes with rounded edges required for the design shown in Fig. 1(b). Figure 2(a) shows an example of nanoelectrodes used for fabrication of our shuttle junctions. All images were taken using a VEECO Multimode IIIa atomic force microscope and WSxM software²⁷ used for making pseudo-3D AFM images.

To assemble shuttle junctions, we initially covered the nanoelectrodes with a monolayer of 1,8-octanedithiol, which have a length of approximately 1.2 nm. Then nominal 20-nm-diameter gold nanoparticles (G1652 Sigma-Aldrich) were adsorbed by immersion of the electrode assembly into aqueous gold sol. An AFM image of the area around the nanogap was taken, and one of the nanoparticles was manipulated into the gap using the AFM tip. Figure 2(d) shows a sequence of AFM images obtained during such a manipulation. Figures 2(b) and 2(c) show AFM images of some of the shuttle junctions. Current-voltage characteristics of the fabricated devices were measured at room temperature in a shielded dry box to protect samples from moisture and to decrease electromagnetic noise.

Figure 3 shows experimental I - V curves for some fabricated shuttle junctions. The experimental I - V curves show an abrupt rise in the current that can be attributed to the onset of shuttle oscillations. However, this happens at significantly higher voltages than predicted (0.16 V) by the theory.¹ The discrepancy is probably related to the fact that in the theoretical model the nanoparticle is connected to the electrodes via two elastic molecules (one on each side). In our devices the nanoparticle is attached through a monolayer of molecules. As the gap between the spherical nanoparticle and an

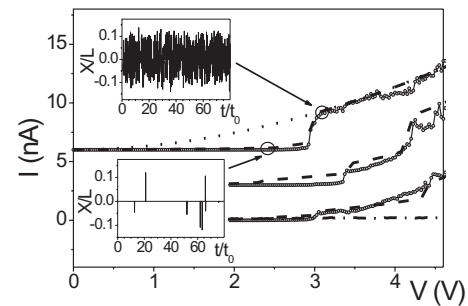


FIG. 3. Experimental (symbols) and simulated (dotted and dashed lines) current-voltage characteristics for shuttle junctions fabricated in the present work. The dotted line corresponds to oscillations in the case of zero pinning and the dashed lines to the case of finite pinning in the system (see text). Insets show the shuttle displacement as a function of time for two points, one of which is below and the other is above the transition into the shuttling regime. The leakage current through a monolayer of octanedithiol molecules is shown by dashed-dotted line.

electrode is nonuniform then some molecules should be overstretched [see inset in Fig. 1(b)]. This would result in “locking” of the nanoparticle at a particular position within the gap so that the nanoparticle is stationary at low voltages. At higher voltages a significant electrostatic force arises that allows the nanoparticle to break bonds with the overstretched molecules and start to oscillate.²⁸ As further experimental proof of this picture, we observed hysteresis of the I - V curves when increasing and then decreasing the applied voltage (inset in Fig. 4). There might be also some other reasons for the restriction of motion of the nanoparticle. For example, as shown in Ref. 9, van der Waals forces may strongly pin the nanoparticle, thus resulting in a strong increase in the shuttling onset and the appearance of hysteresis.

To simulate effects which might restrict the motion of the particle, we have added a pinning potential to the theoretical model¹ and found that the simulated I - V curves (dashed lines in Fig. 3) give much better fit to our experimental results than without pinning (dotted line in Fig. 3). For simulations of the nanoparticle dynamics we used the model proposed in Refs. 1 and 29, with the addition of a potential U :

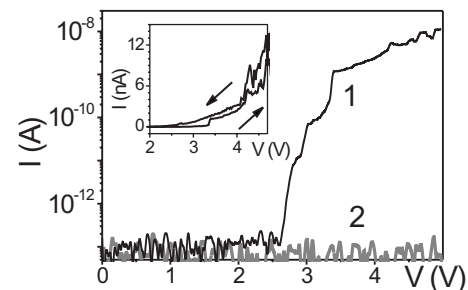


FIG. 4. To prove that current does flow through the nanoparticle in the shuttling regime (curve 1) we removed the nanoparticle from the gap using the AFM tip. This resulted in a drop in the current through the device of several orders of magnitude (curve 2). Inset shows the hysteric behavior of I - V curves obtained for a working shuttle junction in regimes of increasing and decreasing applied voltage.

$\alpha d^2x/dt^2 + dx/dt + \omega_0^2 x = nu + 4n^2x - U'$. Here the first term describes the particle inertia with dimensionless mass α , the second term is related to the viscous force, and the third term is associated with the elastic force having the dimensionless rigidity ω_0^2 . The right-hand side describes both the electrostatic force acting on the nanoparticle carrying n electrons (where the dimensionless voltage u is normalized by the Coulomb blockade threshold V_c) and the pinning force which is described by the dimensionless potential U with the prime denoting a spatial derivative. We used the simplest parabolic potential; i.e., $U' = F_c x/d$ for $|x| < d$ and 0 otherwise. Here, F_c is the maximum pinning force and d is the size of the pinning trap. The position of the particle x (the central position corresponds to $x=0$) is normalized by $2L$ where $L \sim 1$ nm is the size of the gap between particle and an electrode, while time t is normalized by a characteristic time t_0 which is determined by viscosity. Electron tunneling is determined by the probabilities $P_{L,R}^\pm$ to jump from either the left (L) or right (R) junction toward either the right (+) or the left (-) during time Δt : $P_{L,R}^\pm = \Delta t \Delta G_{L,R}^\pm / \{e^2 R_{L,R}^\pm [1 - \exp(-\Delta G_{L,R}^\pm / E_T)]\}$, where $\Delta G_{L,R}^\pm$ is the decrease in the free energy in the system as an electron tunnels; tunneling resistance $R_{L,R}^\pm$ obeys exponential law $R_L(x) = R_R(-x) = R_0 \exp(xL/\lambda)$ with a constant R_0 (which was taken 1 TOhm) and the tunneling length λ is less or about 0.5 Å, and $E_T = k_B T$ is the thermal energy with $T = 300$ K. It is important to stress that the energy change $\Delta G_{L,R}^\pm$ depends on the particle position as $\Delta G_{L,R}^\pm = 0.5eV_c(1 - 4x^2) [\pm 2jn \pm u / (1 + 2jx)]$ with $j = \pm 1$ for (R/L) indices. At first glance, these equations contain many adjustable parameters. However, we can estimate most of them. Indeed, V_c is fixed by the capacitance of the shuttle and is about 0.16 V. Parameter α is determined by the shuttle mass $M = 8 \times 10^{-20}$ kg: $\alpha = L^2 M / eV_c t_0^2 = 3/t_0^2$ if t_0 measured in nanoseconds. As measured in Ref. 30, the elastic constant for one molecule is about 5×10^{-3} N/m. Assuming that shuttle is linked by ten molecules we estimate the elastic constant K as 5×10^{-2} N/m, resulting in $\omega_0 = (KL^2 / eV_c)^{1/2} = 1.4$. So we have only three fitting parameters F_c , d , and t_0 which are determined by pinning and viscosity, respectively.

Damping (or equally t_0) can be readily extracted from the slope of the I - V curves at large enough voltages ($V > V_c$). We found $t_0 \approx 2000$ ns for all three experimental curves. Note that damping only slightly affects the threshold value (see, e.g., Fig. 3 in Ref. 9) and cannot be responsible for the high-voltage thresholds found in our experiments. This is clearly seen in Fig. 3 where two fitting curves with and without pinning (all other parameters are the same) are shown for the top experimental I - V dependence. Unfortunately, we could not find a way to determine the pinning profile from experiments. The specific shape of the electrodes does not allow association of this pinning with, say, image charges studied in Ref. 9. Therefore, we decided to use a pointlike pinning to minimize the number of adjustable parameters. Fitting the onset of shuttling, we obtained $(F_c, d) = (150, 10^{-5}), (95, 4 \times 10^{-5}), (130, 4 \times 10^{-5})$ for Fig. 4 (top, middle, and bottom dashed curves, respectively, also compare with zero pinning curve shown by dotted line). Note that we also tried to vary the location of the pinning center and found that this results in a rescaling of (F_c, d) . For simplicity, we assumed that the

pinning center is located in the middle of the sample.

At low voltages, the shuttle is in the locked state and the electrical current through the device is due to sequential tunneling of electrons from the source electrode to the nanoparticle and then to the drain electrode. The shuttle junction in this regime is similar to a double tunnel junction. As the voltage is increased the electrostatic force applied to the nanoparticle will grow, first, because more electrons will reside on the nanoparticle and, second, because larger electric field will be applied to it. Eventually a voltage will be reached where the nanoparticle can escape its locked position and start to vibrate.³¹

The amplitude of vibrations will increase until a balance is achieved between dissipated and adsorbed energies. The number of electrons transferred in one cycle will depend on the capacitance, C , of the shuttle, its vibration frequency, and applied voltage, V . Transition to the shuttling regime manifests itself as a sudden increase in the transmitted current.

A comparison of the experimental and simulated I - V curves enabled us to estimate several important parameters of our shuttle devices. Naively, the maximum number of electrons carried by a nanoshuttle is determined by the condition $N_{\max} = [CV/e + 0.5]$.¹ For larger N , the addition of an extra electron becomes energetically unfavorable. For our gold spherical particles with radius $R = 10$ nm, we estimate self-capacitance as $C = 4\pi\epsilon_0 R \sim 10^{-18}$ F, which provides N_{\max} of about 20 electrons for the applied voltage of ~ 3 V. However, if damping is strong then the shuttle may carry fewer electrons as it will not be able to approach an electrode close enough to get the maximum load. The actual number of electrons sitting on the nanoshuttle will fluctuate within a certain range ($N - \Delta N, N + \Delta N$) thus producing fluctuations in the average electrostatic force applied to the particle. The shuttle starts to oscillate as soon as the electrostatic force for $N + \Delta N$ electrons exceeds the pinning force. However, the nanoparticle can get stuck if the occupation number reduces (e.g., $N - \Delta N$) due to fluctuations. This sticking may be due to the factors mentioned above, such as the van der Waals force or due to rebinding of “overstretched” molecules to the electrodes or nanoparticle. Such events produce occasional breaks in shuttling and the associated sudden steps in the I - V curves, which are clearly seen in both experimental and simulated curves. Three simulation curves which were obtained for slightly different values of the pinning force and the size of the pinning trap are presented in Fig. 3. As can be seen, these small variations in the pinning parameters have significant effect on the shape of the I - V curves and the number of the steps observed. Two insets in Fig. 3 show shuttle displacement as a function of time at points below and above the depinning threshold, at $V = 3$ V, for one of the simulated I - V curves. Below the threshold, the nanoparticle is making rare attempts to oscillate when the fluctuating number of electrons accumulated on the particle becomes large enough. However, it becomes retrapped again as soon as the number of electrons sitting on it fluctuates to a lower value. This process, a “precursor” to the depinning, produces a small current below 3 V. Above the threshold the nanoparticle oscillates but the oscillations are quite irregular and, importantly, the amplitude of displacement of the nanoparticle varies significantly. The nanoparticle rarely approaches the

electrodes closely enough to gain the maximum charge ($N_{\max}=20$ for 3 V), and on average it carries only four to seven electrons.

Finally, in order to prove that the measured current in our experiments was transferred through the nanoparticle rather than being caused by leakage, we have performed several tests. First of all, we checked that octanedithiols have a high leakage resistance. It is known that results obtained for conductance of organic monolayers strongly depend on geometry of the probes and environment.^{32,33} So we tried to keep these parameters the same as in our studies of shuttle junctions and prepared test samples by depositing from solution 20 nm gold nanoparticles on an Au $\langle 111 \rangle$ surface, preliminarily coated with a monolayer of octanedithiols. Then, using the tip of a scanning tunneling microscope, we applied voltage between individual nanoparticles and the Au $\langle 111 \rangle$ surface and measured current through the layer of molecules. The observed currents did not exceed 0.25 nA at 5 V (dash-dotted line in Fig. 3), which is much smaller than the current transferred by shuttles. We also compared characteristics of a working shuttle device (curve 1 in Fig. 4) with the same

device but from which we carefully removed the nanoparticles (curve 2 in Fig. 4). After the nanoparticle was removed, current through the device dropped to the level of noise.

In conclusion, we fabricated shuttle junctions consisting of a 20 nm gold nanoparticle attached to two electrodes through a monolayer of flexible organic molecules. Measured current-voltage characteristics have been compared with results of computer simulations and found to be in correspondence with the shuttling mechanism of charge transport.

The work was funded by the EPSRC-GB under Grant No. GR/S47793/01 and was also partially supported by the EPSRC-GB via Grant No. EP/D072581/1. R.W.F. thanks the Innovative electronic Manufacturing Research Council (IeMRC) for the support (Grant No. GR/T07549). S.S. acknowledges DML, RIKEN for access to the computer facilities. We are very grateful to R. I. Shekhter, L. Y. Gorelik, and M. Jonson for fruitful discussions.

*Corresponding author; s.gordeev@bath.ac.uk

¹L. Y. Gorelik, A. Isacsson, M. V. Voinova, B. Kasemo, R. I. Shekhter, and M. Jonson, *Phys. Rev. Lett.* **80**, 4526 (1998).

²K. K. Likharev, *IEEE Trans. Magn.* **23**, 1142 (1987).

³D. V. Averin and Y. V. Nazarov, *Phys. Rev. Lett.* **65**, 2446 (1990).

⁴T. M. Eiles, G. Zimmerli, H. D. Jensen, and J. M. Martinis, *Phys. Rev. Lett.* **69**, 148 (1992).

⁵L. Y. Gorelik, A. Isacsson, Y. M. Galperin, R. I. Shekhter, and M. Jonson, *Nature (London)* **411**, 454 (2001).

⁶A. D. Armour and A. MacKinnon, *Phys. Rev. B* **66**, 035333 (2002).

⁷R. I. Shekhter, Yu. Galperin, L. Y. Gorelik, A. Isacsson, and M. Jonson, *J. Phys.: Condens. Matter* **15**, R441 (2003).

⁸K. D. McCarthy, N. Prokof'ev, and M. T. Tuominen, *Phys. Rev. B* **67**, 245415 (2003).

⁹T. Nord and A. Isacsson, *Phys. Rev. B* **69**, 035309 (2004).

¹⁰A. Yu. Smirnov, L. G. Mourokh, and N. J. Horing, *Phys. Rev. B* **69**, 155310 (2004).

¹¹F. Pistolesi and R. Fazio, *Phys. Rev. Lett.* **94**, 036806 (2005).

¹²A. Donarini, T. Novotny, and A.-P. Jauho, *New J. Phys.* **7**, 237 (2005).

¹³F. Rütting, A. Erbe, and C. Weiss, *New J. Phys.* **7**, 240 (2005).

¹⁴D. A. Rodrigues and A. D. Armour, *New J. Phys.* **7**, 251 (2005).

¹⁵F. Pistolesi and R. Fazio, *New J. Phys.* **8**, 113 (2006).

¹⁶M. R. Wegewijs and K. C. Nowack, *New J. Phys.* **7**, 239 (2005).

¹⁷D. W. Utami, H.-S. Goan, C. A. Holmes, and G. J. Milburn, *Phys. Rev. B* **74**, 014303 (2006).

¹⁸R. H. Blick, A. Erbe, H. Krömmner, A. Kraus, and J. P. Kotthaus, *Physica E* **6**, 821 (2000).

¹⁹R. G. Knobel and A. N. Cleland, *Nature (London)* **424**, 291

(2003).

²⁰A. Erbe, C. Weiss, W. Zwerger, and R. H. Blick, *Phys. Rev. Lett.* **87**, 096106 (2001).

²¹D. V. Scheibe and R. H. Blick, *Appl. Phys. Lett.* **84**, 4632 (2004).

²²H. Park, J. Park, A. K. L. Lim, E. H. Anderson, A. P. Alivisatos, and P. L. McEuen, *Nature (London)* **407**, 57 (2000).

²³M. P. Blencowe, J. Imbers, and A. D. Armour, *New J. Phys.* **7**, 236 (2005).

²⁴A. A. Clerk and S. Bennett, *New J. Phys.* **7**, 238 (2005).

²⁵L. Y. Gorelik, D. Fedorets, R. I. Shekhter, and M. Jonson, *New J. Phys.* **7**, 242 (2005).

²⁶L. Y. Gorelik, S. I. Kulinich, R. I. Shekhter, M. Jonson, and V. M. Vinokur, *Phys. Rev. B* **71**, 035327 (2005).

²⁷I. Horcas, R. Fernández, J. M. Gómez-Rodríguez, and J. Colchero, *Rev. Sci. Instrum.* **78**, 013705 (2007).

²⁸Our order of magnitude calculations show that the voltage of 3 V is required to break ten bonds.

²⁹T. Nord, L. Y. Gorelik, R. I. Shekhter, and M. Jonson, *Phys. Rev. B* **65**, 165312 (2002).

³⁰Y. Sakai, T. Ikehara, T. Nishi, K. Nakajima, and M. Hara, *Appl. Phys. Lett.* **81**, 724 (2002).

³¹See an animation of this scenario on the website <http://www.lboro.ac.uk/departments/ph/research/animations/Shuttle1.swf>

³²X. D. Cui, A. Primak, X. Zarate, J. Tomfohr, O. F. Sankey, A. L. Moore, T. A. Moore, D. Gust, G. Harris, and S. M. Lindsay, *Science* **294**, 571 (2001).

³³D. P. Long, J. L. Lazorcik, B. A. Mantoath, M. H. Moore, M. A. Ratner, A. Troisi, Y. Yao, J. W. Ciszek, J. M. Tour, and R. Shashidhar, *Nature Mater.* **5**, 901 (2006).